

## Rhizaria in the oligotrophic ocean exhibit clear temporal and vertical variability.

Alex Barth<sup>\*1,2</sup>, Leocadio Blanco-Berical<sup>3</sup>, Rod Johnson<sup>3</sup> and Joshua Stone<sup>1</sup>

1. University of South Carolina, Biological Sciences, 700 Sumter St 401, Columbia, SC 29208
2. University of Texas at Austin, Marine Science Institute, 750 Channel Drive, Port Aransas, Texas, USA
3. Arizona State University, School of Ocean Futures, Bermuda Institute of Ocean Sciences 17 Biological Station, St Georges, GE 01

### Abstract

Recently studies have shown that Rhizaria, a super-group of marine protists, have a large role in pelagic ecosystems. They are unique in that they construct mineral tests out of silica, calcium carbonate, or strontium sulfate. As a consequence, Rhizaria can have large impacts on the ocean's cycling of carbon and other elements. However, less is known about Rhizaria ecology or their role in the pelagic food-web. Some taxa, like certain Radiolarians, are mixotrophic, hosting algal symbionts. While other taxa are flux-feeders or even predatory carnivores. Some prior research has suggested that Rhizaria will partition vertically in the water column, likely due to different trophic strategies. However, very few studies have investigated their populations over extended periods of time. In this study, we present data investigating Rhizaria abundance and vertical distribution from over a year of monthly cruises in the Sargasso Sea. This study represents the first quantification of Rhizaria throughout the mesopelagic zone in an oligotrophic system for an extended period of time. We use this data to investigate the hypothesis that Rhizaria taxonomic groups will partition due to trophic mode. We also investigate how their abundance varies in accordance with environmental parameters. Rhizaria abundance was quantified using an Underwater Vision Profiler (UVP5), an in-situ imaging device. Ultimately, we show that different Rhizaria taxa will have unique vertical distribution patterns. Models relating their abundance to environmental parameters have mixed results, yet particle concentration is a common predictive variable, supporting the importance of heterotrophy amongst many taxa.

## <sup>2</sup> Introduction

<sup>3</sup> Rhizaria are an extremely diverse super-group of single-celled organisms which occupy a wide range of  
<sup>4</sup> habitats. Planktonic Rhizaria include Foraminifera, Radiolaria (including Acantharea and Collodaria) and  
<sup>5</sup> Phaeodaria, all of which are observed throughout the global ocean (Biard et al., 2016; Laget et al., 2024)  
<sup>6</sup> . While the taxonomy of these organisms has recently undergone several reclassifications (Biard, 2022a),  
<sup>7</sup> their presence in ocean ecosystems has been long known to oceanographers. Some of the earliest records  
<sup>8</sup> of their existence are from oceanographic expeditions in the 19th century (Haekel, 1887). Rhizaria are  
<sup>9</sup> unique members of the plankton and protist community because they can reach large sizes (up to several  
<sup>10</sup> mm in diameter) and they construct intricate mineral skeletons out of either silica, strontium, or calcium  
<sup>11</sup> carbonate (Biard, 2022a; Kimoto, 2015; Nakamura and Suzuki, 2015; Suzuki and Not, 2015). Despite their  
<sup>12</sup> noticeable morphology and global distribution, Rhizaria were largely understudied throughout the 20th  
<sup>13</sup> century. Fragile organisms like Rhizaria are difficult to adequately study because they can be destroyed  
<sup>14</sup> through standard zooplankton sampling techniques and preserve poorly. A number of studies in the late  
<sup>15</sup> 1900s did employ alternative techniques to quantify Rhizaria including diaphragm pumps (Michaels, 1988)  
<sup>16</sup> or blue-water SCUBA collections (Bijma et al., 1990; Caron et al., 1995; Caron and Be, 1984). However, the  
<sup>17</sup> bulk of Rhizaria research was constrained to sediment traps or paleontological studies of sediment (Boltovskoy  
<sup>18</sup> et al., 1993; Takahashi et al., 1983).

<sup>19</sup> Recently, the advent of molecular techniques and *in situ* imaging tools have ignited a renewed focus on  
<sup>20</sup> Rhizaria in pelagic ecosystems (Caron, 2016). Molecular tools have shed light on Rhizaria taxonomy (Biard,  
<sup>21</sup> 2022a), distribution (Blanco-Bercial, 2020; Sogawa et al., 2022), ecology (Decelle et al., 2012; Nakamura  
<sup>22</sup> et al., 2023), biogeochemical roles (Gutierrez-Rodriguez et al., 2019; Laget et al., 2024), and metabolism  
<sup>23</sup> (Cohen et al., 2023). Yet, despite the excellent taxonomic resolution provided by molecular approaches, they  
<sup>24</sup> do not provide a truly quantitative metric for estimating Rhizaria abundance or biomass. *In situ* imaging

25 tools however, offer the ability to observe organisms in the natural state and quantify their abundance (Barth  
26 and Stone, 2024; Ohman, 2019). Biard et al. (2016) utilized *in situ* imaging at a global scale to suggest  
27 large (>500 $\mu\text{m}$  diameter) Rhizaria were substantial contributors to the ocean carbon standing stock. While  
28 more recent calculations suggest lower carbon contribution (Laget et al., 2024), Rhizaria nonetheless have  
29 substantial influences on biogeochemical cycling. This influence is due to their unique mineral skeletons and  
30 ability to repackage small particles into larger, fast sinking ones (Ikenoue et al., 2019). Thus, some Rhizaria  
31 may play substantial roles in ocean export through their interception of sinking particles (Laget et al., 2024;  
32 Stukel et al., 2018). However, Rhizaria ecology is poorly understood (Biard, 2022a) and their ecological roles  
33 are likely more than diverse than simple particle interception.

34 The ecological role of Rhizaria in plankton communities is complicated due to the fact different taxa can  
35 exhibit very different trophic modes. Many Rhizaria are strictly heterotrophic (Biard, 2022a), yet their  
36 feeding modes can be quite varied. Phaeodaria are largely thought to be flux-feeders, collecting and feed-  
37 ing on sinking particles (Gowing, 1989). Alternatively, Retaria can be either exclusively heterotrophic or  
38 mixotrophic, utilizing photosynthetic algal symbionts (Anderson, 2014; Decelle et al., 2015). Mixotrophic  
39 Foraminifera host a variety of endosymbiont partners (Decelle et al., 2015; Lee, 2006), which are thought to  
40 support early and adult life stages and significantly contribute to total primary productivity (Kimoto, 2015).  
41 Still, Foraminifera are omnivorous, possibly even predominately carnivorous, with several studies suggesting  
42 that they can be effective predators (Anderson and Bé, 1976; Gaskell et al., 2019), mainly consuming live  
43 copepods (Caron and Be, 1984). Radiolaria have several lineages, many of which host symbionts (Biard,  
44 2022b). Amongst Radiolaria, arguably the most widespread are Collodaria who can be either large solitary  
45 cells or form massive colonies, up to several meters in length (Swanberg and Anderson, 1981). All known  
46 Collodaria species host dinoflagellate symbionts (Biard, 2022b) and can contribute substantially to primary  
47 productivity, particularly in oligotrophic ocean regions (Caron et al., 1995; Dennett et al., 2002). This

48 Collodaria-symbiont association has been suggested as a reason for their high abundances throughout the  
49 photic zone of oligotrophic environments globally (Biard et al., 2017, 2016). A few Acantharea (Radiolaria  
50 order) clades host algal symbionts (Biard, 2022b; Decelle et al., 2012), notably with two clades forming an  
51 exclusive relationship with *Phaeocystis*. However, globally, Acantharea are less abundant than Collodaria  
52 (Biard, 2022a) and contribute less to total primary productivity (Michaels et al., 1995). This may be due  
53 to the fact several clades of Acantharea are cyst-forming and strictly heterotrophs (Biard, 2022b; Decelle et  
54 al., 2013). Furthermore, Mars Brisbin et al. (2020) documented apparent predation behavior in Acantharea  
55 near the surface, suggesting that there may be a larger reliance on carnivory.

56 Given the high abundances, yet diverse trophic strategies found among Rhizaria taxa, it is reasonable to  
57 expect some form of niche partitioning. A number of studies do suggest evidence for vertical zonation  
58 between Rhizaria groups according to various trophic strategies. Taxon-specific studies of Radiolaria suggest  
59 they may be restricted to the euphotic zone (Boltovskoy, 2017; Michaels, 1988). Although some studies  
60 report Acantharea in deeper waters (Decelle et al., 2013; Gutiérrez-Rodríguez et al., 2022), Phaeodaria,  
61 alternatively, are generally found beyond depths where light can sustain photosynthesis, but they can feed  
62 on sinking particles (Laget et al., 2024; Stukel et al., 2018). In an imaging-based study of the whole Rhizaria  
63 community, Biard and Ohman (2020) noted clear patterns in vertical zonation which largely corresponded  
64 to different trophic roles. Protists communities, including Rhizaria, have been described to partition along  
65 autotroph-mixotroph-heterotroph gradients with increasing depth in the water column (Blanco-Bercial et  
66 al., 2022; Laget et al., 2024). Yet, few studies have made direct attempts to relate Rhizaria abundances  
67 to environmental factors (Biard and Ohman, 2020). In part, this is due to the fact few studies have been  
68 able to sample Rhizaria in the same location over a consistent timeframe (Boltovskoy et al., 1993; Gutiérrez-  
69 Rodríguez et al., 2022; Hull et al., 2011; Michaels et al., 1995; Michaels, 1988). Furthermore, very few studies  
70 have utilized *in situ* imaging, arguably the best method for quantifying Rhizaria, to consistently throughout

71 the full mesopelagic (Laget et al., 2024) . Given this lack of information, there are many unknowns with  
72 respect to Rhizaria ecology, seasonality and phenology across different groups.

73 In this study, we present a comprehensive assessment of large Rhizaria abundance measured for over a year  
74 from regularly occurring cruises at monthly intervals. We utilized an *in situ* imaging approach to facilitate  
75 abundance calculations. With this dataset, we address two critical aims. 1) Quantifying of large Rhizaria  
76 throughout the epipelagic (0-200m) and mesopelagic (200-1000m) over the course of an annual cycle. These  
77 data were collected in the Sargasso Sea, and represents the first study of its kind in an oligotrophic sys-  
78 tem; and 2) We aim to test the hypothesis that Rhizaria exhibit niche partitioning according to trophic  
79 roles. This hypothesis has several implications, including vertical zonation, as seen in prior studies, but also  
80 that environmental variables related to trophic strategy will explain abundance patterns. Specifically, au-  
81 totrophic/mixotrophic taxa will correspond to variables related to autotrophy (chl-a concentration, primary  
82 productivity, local DO maxima) and other rhizaria will correspond to factors which promote heterotrophy  
83 (particle concentration, flux, and local DO minima).

## 84 Methods

### 85 Oceanographic sampling

86 Data were collected in collaboration with the Bermuda Atlantic Time-series Study (Lomas et al., 2013;  
87 Michaels and Knap, 1996) on board the R/V Atlantic Explorer. Cruises were conducted at approximately  
88 monthly intervals. Rhizaria individuals were sampled using the Underwater Vision Profiler 5 (UVP) (Picheral  
89 et al., 2010). The UVP5 is an in-situ camera used to capture plankton and particle images and has been well  
90 established to accurately quantify large Rhizaria abundance (Barth and Stone, 2022; Biard et al., 2016; Biard  
91 and Ohman, 2020; Drago et al., 2022; Llopis Monferrer et al., 2022; Panaïotis et al., 2023; Stukel et al., 2019;

92 Stukel et al., 2018). The UVP5 was mounted to the sampling rosette and collected data autonomously on  
93 routine casts, from which only the downcast data are utilized. The UVP5 was deployed from June-September  
94 2019 then from October 2020 - January 2022, during which time the BATS region was sampled for 3-5 days  
95 at monthly intervals (see sampling details in Supplemental Table 1). Casts were filtered to only include data  
96 collected in the BATS region, far offshore of Bermuda in the Sargasso Sea (approximately  $31.0^{\circ}N$ - $32.5^{\circ}N$ ,  
97  $64.25^{\circ}W$ - $63^{\circ}W$ ; Supplemental Figure 1). In general, casts extended to either 200m, 500m, or 1200m deep,  
98 with a few extended into the bathypelagic (4500m). However, Rhizaria were only typically found in large  
99 abundances throughout the epipelagic and mesopelagic zones. As such, we limit this study to results from  
100 the upper 1000m of the water column.

101 A variety of biotic and abiotic data were collected during each BATS cruise. The UVP5 provided particle  
102 count data at a high-frequency from each cast. Particle concentration, as a proxy for prey field (Whitmore  
103 and Ohman, 2021), was calculated from this data for all particles  $184\mu m$  -  $900\mu m$ . The lower size range  
104 was set by what could be reliably sampled by the UVP5's pixel resolution ( $>2px$ ; 0.092mm per pixel) and  
105 the upper size range was set to below the size of observable Rhizaria yet large enough to be inclusive of  
106 particles on which some Rhizaria may feed. For each UVP cast supporting continuous profiles of the CTD  
107 parameters salinity, temperature, and auxiliary CTD channels; Dissolved Oxygen (DO), *in situ* chlorophyll  
108 fluorescence were measured at 24Hz using the BATS CTD package. On select casts, Niskin bottles were  
109 used to collect bacterial abundance estimates (via epifluorescence microscopy) as well as measure inorganic  
110 nutrients ( $NO_3$ , and  $Si$  as silicate/silicic acid) at discrete depths. On each cruise, flux estimates of total  
111 mass, organic carbon, and nitrogen were also collected using sediment traps; in the present study we utilized  
112 flux to the mesopelagic as the flux at 200m. Also primary productivity was estimated through measuring  $^{14}C$   
113 uptake rates from *in situ* incubations. For full descriptions of the BATS sampling program and methods,  
114 see Knap et al. (1997) and Lomas et al. (2013) for a review. Additionally, data can be viewed online

115 (<https://bats.bios.asu.edu/bats-data/>).

116 Environmental data were processed to match the format of the Rhizaria abundance estimates (see below).

117 CTD data were collected at higher frequency than the UVP (24Hz vs 15Hz respectively), so these data were

118 averaged within matching bins to the UVP5 data. Data from Niskin bottles were first linearly interpolated

119 in depth at 1m resolution then time averaged over the cruise, then subsequently averaged into matching

120 bins as the UVP5 data. Primary productivity estimates were depth integrated throughout the euphotic zone

121 (0-140m).

## 122 Rhizaria imaging processing and abundance quantification

123 Individual vignettes of Rhizaria images were identified using the classification platform EcoTaxa (Picheral  
124 et al., n.d.). Data were pre-sorted utilizing a random-forest classifier and pre-trained learning set. Taxo-  
125 nomic classification were done based on morphological parameters measured in Zooprocess (Gorsky et al.,  
126 2010), which includes parameters such as major axis, equivalent spherical diameter (ESD), and grey val-  
127 ues. While there are sparse taxonomic guides for *in situ* images of Rhizaria, identification largely relied  
128 on descriptions in (Nakamura and Suzuki, 2015; Suzuki and Not, 2015; and Biard and Ohman, 2020). Us-  
129 ing the aforementioned sources and publicly available EcoTaxa projects, we constructed a guide accessible  
130 at: [https://thealexbarth.github.io/media//Project\\_Items/Oligotrophic\\_Community/ecotaxa\\_UVP-guide-  
stone-lab.pdf](https://thealexbarth.github.io/media//Project_Items/Oligotrophic_Community/ecotaxa_UVP-guide-stone-lab.pdf). Broadly, Rhizaria were classified as Foraminifera, Radiolaria (Acantharea or Collodaria), or  
132 as a variety of Phaeodaria families (Figure 1). When identification could not be confidently made between  
133 a few candidate taxa, a less specific label was used. As a result, we have data from “unidentified Rhizaria”,  
134 which typically were vignettes not distinguishable between Aulacanthidae or Acantharea or “unidentified  
135 Phaeodaria”, which are clearly Phaeodaria but not distinguishable into a family.

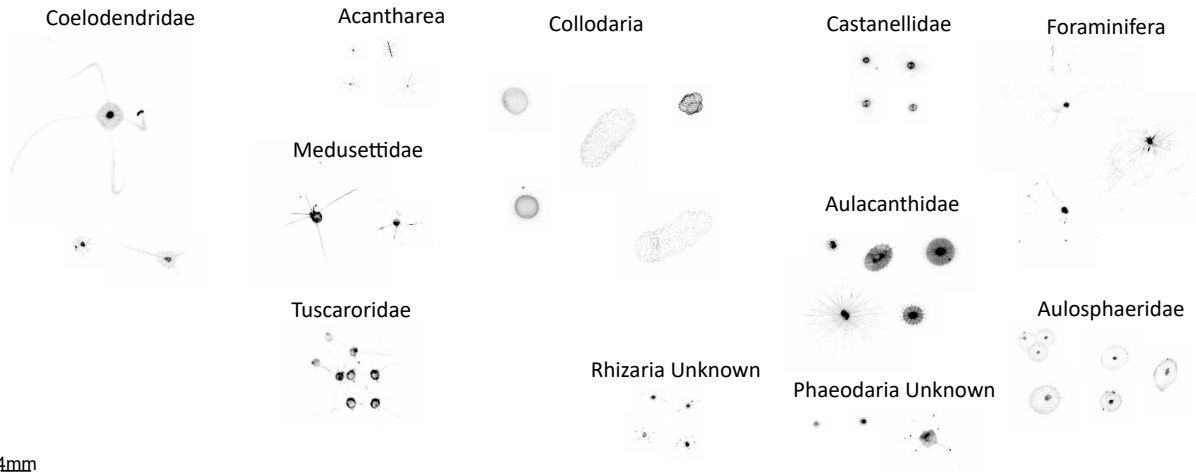


Figure 1: Example images of different Rhizaria taxa as collected by UVP5 imaging. 4mm scale bar shown in lower right. All vignettes are same scale

136 The UVP5 samples at  $\sim 15\text{Hz}$  rate as it descends the water column and records the exact position of each  
 137 particle larger than  $600\mu\text{m}$  (ESD). However, identified rhizaria ranged from a  $934\mu\text{m}$  ESD Aulacanthidae  
 138 cell to a Collodarian colony over 10mm in diameter. To confirm that the UVP5 was sampling adequately  
 139 across all size ranges, a normalized biomass size spectrum (NBSS) slope was constructed to identify a  
 140 drop-off which would indicate poor-sampling at the small size range (Barth and Stone, 2024; Lombard et  
 141 al., 2019). However, it was evident from this analysis that all size ranges were adequately sampled across  
 142 the size range (Supplemental Figure 2) so no data were excluded. The UVP5 reports the exact depth at  
 143 which a particle is recorded, however to estimate abundance, observations must be binned over fixed depth  
 144 intervals. Our deployments had variable descent depths and speeds with more casts descending to 500m than  
 145 1000m and descents quicker through the epipelagic than the mesopelagic (see Barth and Stone (2022) for an  
 146 extended discussion of UVP5 data processing). For the present study, Rhizaria abundances were estimated  
 147 in 25m vertical bins, which offer a moderate sampling volume per bin (average  $0.948\text{m}^3$  in the epipelagic  
 148 and  $0.589\text{m}^3$  in the mesopelagic; Supplemental Table 1) while still maintaining ecologically relevant widths.

149 However, concentrations in a 25m bin would need to be greater than  $2.428 \text{ ind. } m^{-3}$  and  $3.912 \text{ ind. } m^{-3}$ , in  
150 the epipelagic and mesopelagic respectively, to fall below a 10% non-detection risk (Barth and Stone, 2024;  
151 Benfield et al., 1996). Because we typically observed many Rhizaria taxa below these concentrations, we  
152 present the 25m binned data to visualize broad-scale average distributions. For quantifying and modelling  
153 Rhizaria abundances, we present integrated abundance estimates, with each cast. Due to the variable descent  
154 depths of the UVP, data are categorized as epipelagic (0-200m), upper mesopelagic (200-500m), and lower  
155 mesopelagic (500-1000m). The average sampling volume integrated through these regions were  $7.59m^2$ ,  
156  $7.06m^2$ , and  $11.77m^2$ , with non-detection thresholds at  $0.30 \text{ ind. } m^{-2}$ ,  $0.33 \text{ ind. } m^{-2}$ , and  $0.20 \text{ ind. } m^{-2}$   
157 respectively. All UVP data processing was done using the `EcotaxaTools` package in R (Barth 2023).

## 158 Modelling environmental controls of Rhizaria abundance

159 Generalized Additive Models (GAMs) were used to assess the relationship between integrated Rhizaria abun-  
160 dance and different environmental factors. GAMs offer the ability to model non-linear and non-monotonic  
161 relationships, which can be particularly useful in assessing ecological relationships (Wood, 2017) and have  
162 been successfully applied to Rhizaria ecology (Biard and Ohman, 2020). The `mgcv` package (Wood, 2001)  
163 was used to construct models relating environmental parameters to each taxonomic group's integrated abun-  
164 dance estimates from each cast. To select the most parsimonious model for each analysis, a backwards  
165 step-wise approach was taken. First, a full model was fit using any term which may be ecologically relevant.  
166 Terms were fit using maximum likelihood with a double penalty approach on unnecessary smooths (Marra  
167 and Wood, 2011). The smoothness parameter was restricted ( $k = 6$ ) to prevent over fitting the models.  
168 Then, the full model was checked for concurvity (a metric indicating high parameter relatedness in GAMs).  
169 If two terms had a high concurvity value ( $>0.8$ ), then two alternative models were constructed each leaving  
170 out one of the related terms. The more parsimonious model of these two was selected using AIC. Once

171 concurvity of terms was reduced, then the model was subjected to the backwards step-wise procedure. At  
172 each iteration, the model term with the lowest F score (least statistically significant) was removed. This  
173 was repeated until all model terms were statistically significant or the  $R^2_{adj}$  was substantially reduced. Mod-  
174 els were fit for each water column region; epipelagic, upper mesopelagic, and lower mesopelagic. In cases  
175 where observations were too sparse for a given taxonomic grouping, models were not run. All code, full  
176 models, and model selection tools are available in open-source scripts, as well as intermediate data products  
177 at <https://github.com/TheAlexBarth/RhizariaSeasonality>.

## 178 Results

### 179 Environmental Variability

180 While the environmental conditions were generally low in variation and oligotrophic, there is considerable  
181 influence from deep winter-mixing and summer stratification as well as secondary influences from mesoscale  
182 eddies which result in spatiotemporal heterogeneity (Lomas et al., 2013; McGillicuddy et al., 1998). Vari-  
183 ability in the water column structure was visible during the study period (Figure 2). This is best evidenced  
184 through the temperature profiles; In the late summer and early fall there was a stratified water column with  
185 high temperatures in the surface (<75m) (Figure 2A) and slightly elevated salinity (Figure 2B). This warm,  
186 stratified period appeared more intense during the few months sampled in 2019. In 2021, we observed the  
187 stratified layer slowly dissipated into the winter months following mixed layer entrainment. There was a  
188 consistent oxygen minimum zone (OMZ) located at about 800m deep (Figure 2C). February 2021 saw a  
189 notable downwelling event, likely due to a passing anti-cyclonic eddy which impacted the local region during  
190 early 2021. During this phase, warmer, oxic water was significantly depressed deeper into the mesopelagic.  
191 This process was reversed in the spring months (March, April) primary due to the interaction of convective

192 mixing and the passing of a strong cyclonic eddy resulting in a deep cold mixed layer. Primary production  
193 was highest during the spring mixing period, evidenced both by *in situ* fluorescence (Figure 2D) and produc-  
194 tivity incubation experiments (Figure 3A). Originating near the surface, the productivity peak moved deeper  
195 throughout the spring and declined into the summer (Figure 2D). However, there was a notable, yet smaller  
196 productivity bump in the late summer and early fall (Figure 3A) which occurred deeper in the epipelagic  
197 (Figure 2D). The particle concentration ( $184\mu m - 900\mu m$ ) was closely coupled to chlorophyll-a patterns.

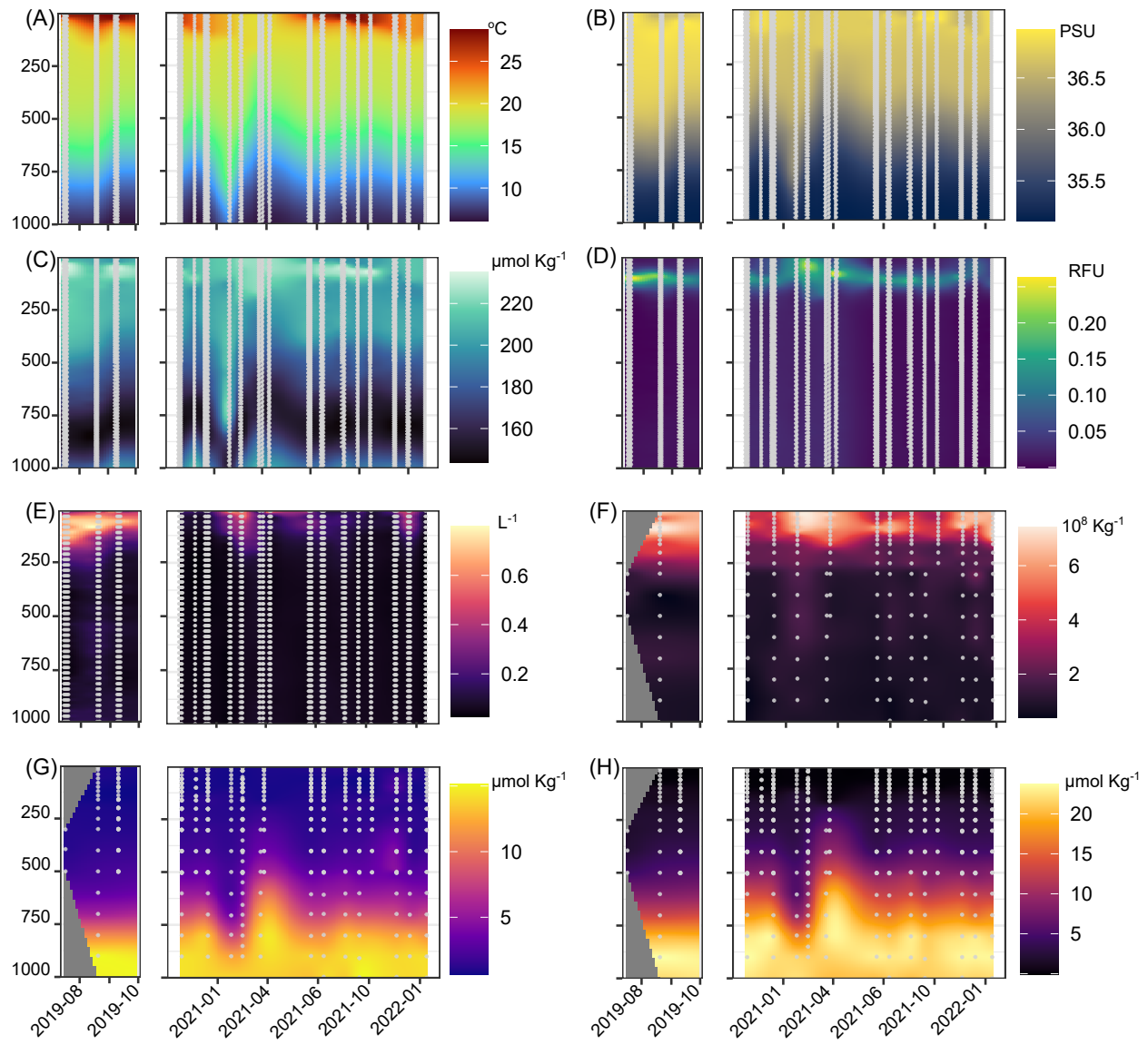


Figure 2: Environmental profiles across time-series of study period. Y axis shows depth in meters. (A) Temperature. (B) Salinity. (C) Dissolved Oxygen. (D) in situ chlorophyll fluorescence. (E) Particle concentration ( $184 - 900 \mu\text{m m}^3$ ). (F) Bacteria Abundance. (G) Silica. (H) Nitrate

198 Overall, particle concentration was high near the surface during the 2021 spring bloom, then moved deeper  
 199 throughout the water column attenuating throughout the lower epipelagic (Figure 2E). Similarly, het-

200 heterotrophic bacteria abundance was closely linked to overall productivity, although there was a more con-  
201 sistent moderate-abundance layer near the top of the mesopelagic (~250m) (Figure 2F). Concurrent with  
202 the secondary fall production peak, there was also higher particle concentration and bacterial abundance in  
203 the later summer and early fall. Interestingly, while primary productivity estimates from July-August were  
204 not that different between 2019 and 2021 (Figure 3A), chlorophyll-a florescence, particle concentration, and  
205 bacterial abundance were much higher in 2019's summer/fall (Figure 2D-F). Inorganic nutrients (*Si* and  
206 *NO<sub>3</sub>*) were generally well stratified, with low concentrations in the epipelagic and increasing throughout the  
207 mesopelagic. However, both nutrients did vary vertically in accordance with the 2021 February downwelling  
208 and spring mixing period (Figure 2G-H). Additionally, in the late fall of 2021, *Si* concentrations were slightly  
209 elevated in the mid-mesopelagic (Figure 2G).

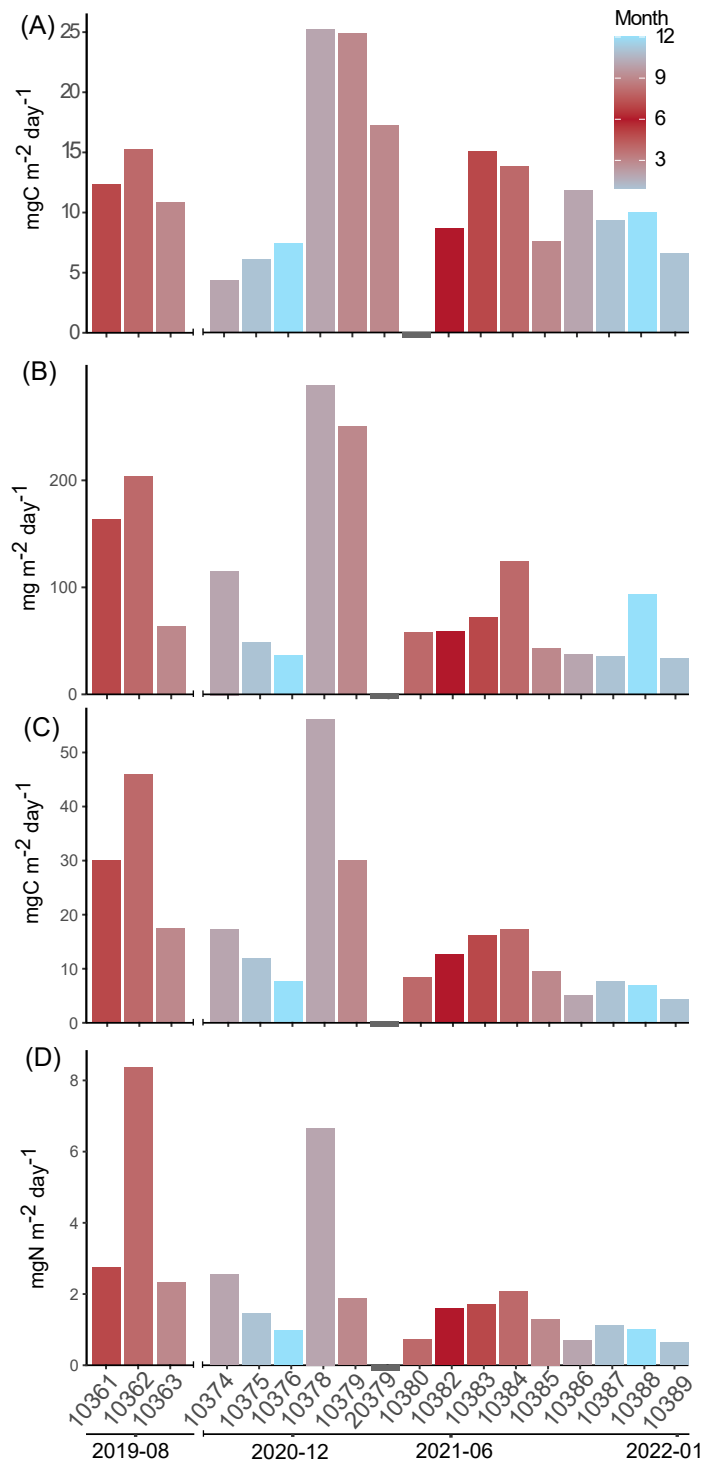


Figure 3: Primary productivity (A) and flux estimates from total mass (B), carbon (C), and nitrogen (D). Values are from monthly cruises with month displayed in corresponding colors. Absent data are shown by grey bar.

210 Overall mass flux to the mesopelagic was highest during the 2021 February downwelling (Figure 3B). Gen-  
211 erally, export was similarly high during March, declining in April then increasing slightly throughout the  
212 summer and early fall. While magnitude was slightly different, this pattern was consistent with total mass,  
213 carbon and nitrogen fluxes (Figure 3B-D). Higher mass, carbon and nitrogen flux also occurred in the 2019  
214 late summer - early fall period.

215 **Rhizaria abundance and distribution**

216 Across all imaged mesozooplankton ( $>900\mu m$ ), Rhizaria comprised a considerable fraction of the total com-  
217 munity. Considering the total abundances of the observational period, Rhizaria comprised on average, 42.6%  
218 of all mesozooplankton abundance (Supplemental Figure 3). Copepods were the second most abundant, com-  
219 prising 35.5% and all other living mesozooplankton were 22%. The large contribution of Rhizaria to the  
220 mesozooplankton community is most prominent in the epipelagic, where they accounted for 47% of all meso-  
221 zooplankton abundance. In the mesopelagic Rhizaria were a smaller fraction, at 38% in the upper layers  
222 (200-500m) and 37% in the deeper mesopelagic (500-1000m).

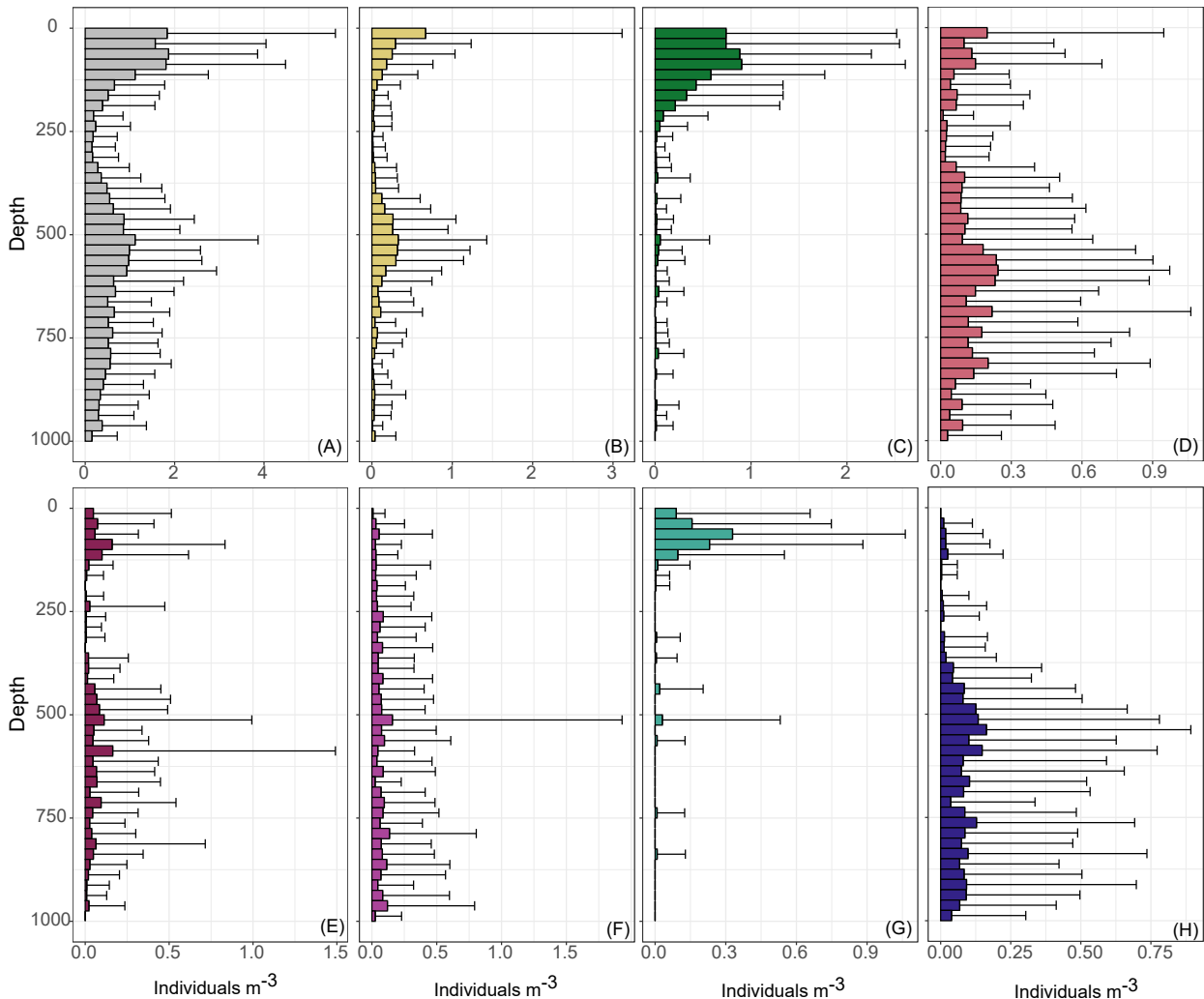


Figure 4: Average abundance of Rhizaria in 25m bins, across entire study period. Shown are total Rhizaria (A), Acantharea (B), Collodaria (C), Aulacanthidae (D), Foraminifera (E), Aulosphaeridae (F), Castanellidae (G), and Coelodendridae (H).

223 Average abundance of all Rhizaria had a bimodal distribution with respect to depth. Total abundance was  
 224 highest just below the surface (0-100m), with secondary, wider peak occurring in the mid mesopelagic (Fig-  
 225 ure 4A). Variation in depth binned abundance was large, likely due to seasonal variability but also increased  
 226 from the detection-risk described in the methods. The vertical distribution pattern and abundance varied

227 considerably across taxonomic groups. Radiolaria were some of the most abundant taxa observed, particu-  
 228 larly in the epipelagic (Figure 4, Figure 5A). Acantharea displayed a bimodal distribution accounting for a  
 229 large portion of the total Rhizaria pattern (Figure 4B, Figure 5). The surface layers were largely comprised of  
 230 Collodaria, whose colonies were abundant (Figure 4C). The most abundant Phaeodaria, Aulacanthidae, also  
 231 had a bimodal pattern with the density was highest in the lower mesopelagic (Figure 4D). Foraminifera had a  
 232 similar bimodal distribution, yet their overall average densities were much lower (Figure 4E). Aulosphaeridae  
 233 had low average density and was nearly homogeneously distributed throughout the water column, although  
 234 slightly lower in the epipelagic (Figure 4F). Castanellidae were the only Phaeodaria who appeared to be  
 235 effectively restricted to the photic zone (Figure 4G). Alternatively, Coelodendridae primarily occurred in  
 236 the lower mesopelagic (Figure 4H). A few individuals from the families Tuscaroridae and Medusettidae were  
 237 also observed in the mesopelagic, yet they were much rarer (data not shown).

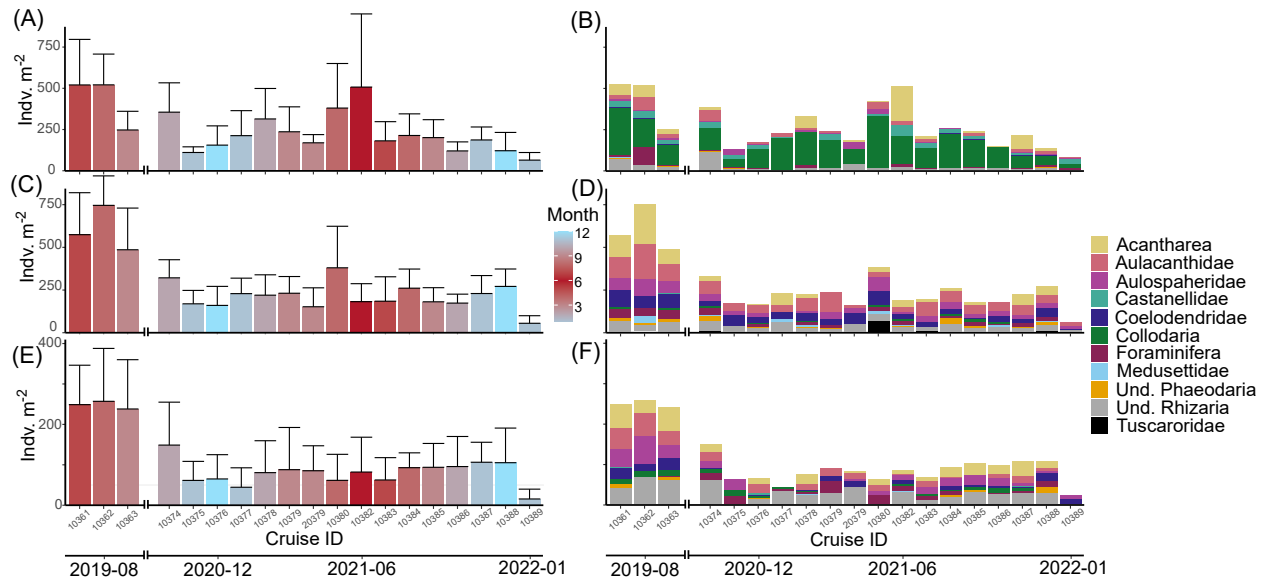


Figure 5: Seasonality of Rhizaria integrated abundance for the epipelagic (0-200m) (A), upper mesopelagic (200-500m) (B), lower mesopelagic (500-1000m) (C). Data shown are the cruise mean integrated abundance in the water column region colored for each taxon.

238 Between the monthly cruises, Rhizaria integrated abundance varied in the epipelagic. Highest average abun-  
239 dance occurred in June 2021 and was lowest during the winter months (Figure 5A). The 2019 later summer  
240 - fall period also had much higher integrated abundance than similar months in 2021. While the majority  
241 of integrated abundance in the epipelagic was consistently attributable to Collodaria, Acanthrea abundance  
242 occurred sporadically and could account for a large portion of the total in some months (Figure 5A). The  
243 mesopelagic integrated abundance was much more consistent across monthly cruises, although average abun-  
244 dance was notably higher in 2019 (Figure 5B, 5C). The community composition in the mesopelagic was more  
245 diverse, mostly comprised of Phaeodaria families. However, Acantharea and unidentified Rhizaria also were  
246 common members of the community (Figure 5B, C).

247 **Body size throughout the water column.**

248 Very few taxa had consistent distributions throughout the water column. Only Acanthrea, Foraminifera,  
249 Aulacanthidae, and Aulosphaeridae were consistently abundant in the epipelagic and mesopelagic. To invest-  
250 ige if the populations or morphologies shifted throughout the water column, we compared the sizes (ESD)  
251 between mesopelagic and epipelagic groups for each taxa. All groups were significantly different on average  
252 (Wilcox Rank Sum p-value <0.001). Acantharea were smaller, on average in the mesopelagic while all other  
253 taxa tended to be larger (Figure 6).

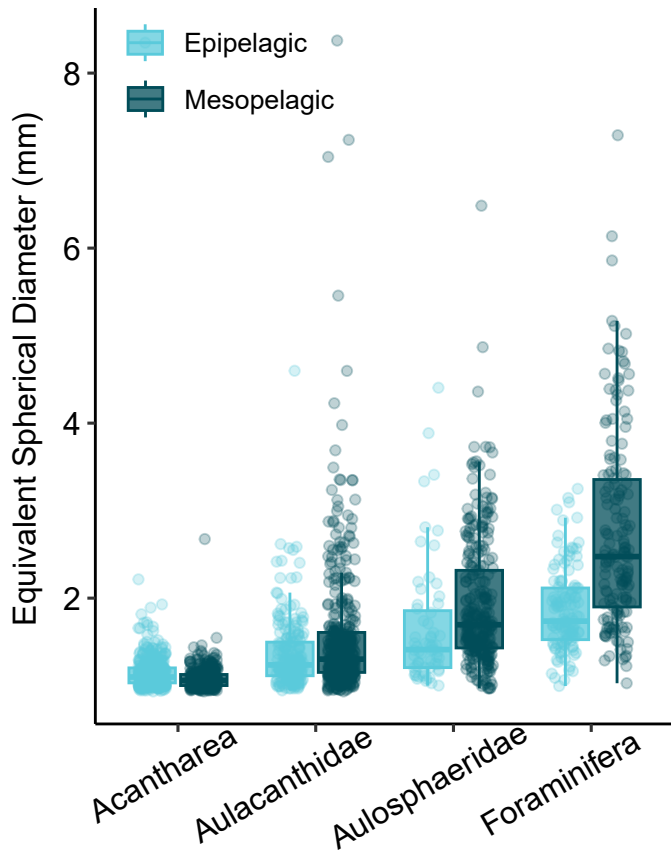


Figure 6: Comparison of average sizes (ESD) amongst Rhizaria taxa which occurred throughout the water column.

**254 Environmental Drivers of Rhizaria Abundance**

**255** For integrated abundance of all Rhizaria, the GAMs produced moderate fits ( $R^2_{adj} = 0.406-0.603$ ) (Table  
**256** 1). In the epipelagic, there were several significant predictor variables (Figure 7A-7G). This included terms  
**257** which are likely indicators of changing water masses; Salinity (7E) and Temperature (7G). The model  
**258** also had parameters related to both heterotrophy (Particle concentration, 7A) and autotrophy (Primary  
**259** production, 7B). However the relationship to particle concentration is weakly increasing trend while the  
**260** primary productivity effect appears to be influenced by a cruise with a high outlier for increased primary

261 productivity. The models for the mesopelagic regions were much more reduced and the only significant  
 262 effects were particle-related terms (particle concentration and mass flux). In the upper mesopelagic (Figure  
 263 7H-7J), final model included N flux, particle concentration and a non-significant effect for Silica. The lower  
 264 mesopelagic (Figure 7K, 7L) only had model effects kept of total mass flux and particle concentration. For  
 265 both the upper and lower mesopelagic, particle concentration had a clear, strong positive relationship (Figure  
 266 7I, 7L).

Table 1: Generalized Additive Model results for integrated total Rhizaria abundance in different regions of the water column. edf = estimated degrees of freedom, F = F-statistic, p = p-value. Models were selected using a backwards-stepwise approach with a retention threshold of  $p = 0.1$  or a large enough reduction in model fit.

Model	Term	edf	F	p
<b>All Rhizaria Epipelagic</b>	Temperature	0.7950	0.492	0.0440
$R^2_{adj} = 0.48$	Salinity	2.4117	5.113	<0.001
	Silica	2.1511	8.601	<0.001
	Bacteria Concentration	0.8870	1.544	<0.001
	Avg Mass Flux	1.4107	0.802	0.0211
	Primary Productivity	1.9280	2.736	<0.001
	Particle Concentration	0.9151	2.136	<0.001
<b>All Rhizaria Upper Mesopelagic</b>	Silica	0.6702	0.404	0.0814
$R^2_{adj} = 0.40$	Avg N Flux	2.9524	3.172	<0.001
	Particle Concentration	3.5568	11.82	<0.001
<b>All Rhizaria Lower Mesopelagic</b>	Avg Mass Flux	2.036	2.953	<0.001
$R^2_{adj} = 0.61$	Particle Concentration	3.819	27.43	<0.001

267 GAMs for individual taxa were much less consistent in their fits (Table 2). This is likely in part due to  
 268 the high number of non-observations for certain taxa. Note that due to low abundances, GAMs were not  
 269 constructed for Tuscaroridae or Medusettidae. Furthermore no, significant terms were found for a model  
 270 with Aulosphaeridae in the epipelagic nor Foraminifera in the mesopelagic.  
 271 Epipelagic Acantharea were explained by several predictor variables and had a good fit ( $R^2_{adj} = 0.539$ ,  
 272 Table 2, Supplemental FIgure 4). Foraminifera had a good fitting GAM in the epipelagic ( $R^2_{adj} = 0.543$ ).  
 273 There were several significant explanatory variables, although the clearest pattern was observed of high  
 274 temperatures associated with more Foraminifera abundance (Table 2, Supplemental Figure 4U). Epipelagic  
 275 Aulacanthidae similarly had several predictor variables which were significant, including both water quality  
 276 parameters and particle/flux predictors (Table 2). There was a weak fit for Collodaria in the epipelagic  
 277 ( $R^2_{adj} = 0.16$ ), although there was a logit-like relationship where higher abundances tended to occur during  
 278 higher DO conditions in the surface waters (Supplemental Figure 4). Castanellidae also had a weak model  
 279 fit in the epipelagic ( $R^2_{adj} = 0.228$ ), although particle concentration was the strongest predictor term (Table  
 280 2, Supplemental Figure 4).

Table 2: Taxa-specific generalized additive models for different regions of the water column.edf = estimated degrees of freedom, F = F-statistic, p = p-value. Models were selected using a backwards-stepwise approach with a retention threshold of p = 0.1 or a large enough reduction in model fit.

Model	Term	edf	F	p
<b>Acantharea Epipelagic</b>	Temperature	0.868	0.380	0.0935
$R^2_{adj}=0.539$	Salinity	2.349	4.646	<0.001
	O2	2.501	5.493	<0.001
	Avg Mass Flux	4.815	22.59	<0.001
	Bacteria	1.608	1.360	0.00945

Model	Term	edf	F	p
	Particle Concentration	0.877	1.414	0.00449
<b>Acantharea Upper Mesopelagic</b>	Avg Mass Flux	1.866	1.220	0.0166
$R_{adj}^2=0.197$	Avg N Flux	2.208	3.100	<0.001
	Primary Productivity	2.382	2.497	<0.001
	Particle Concentration	0.724	0.521	0.0437
<b>Acantharea Lower Mesopelagic</b>	Temperature	1.958	2.986	<0.001
$R_{adj}^2=0.496$	Avg N Flux	1.513	1.565	0.0037
	Primary Productivity	0.856	1.153	0.0045
	Particle Concentration	1.661	8.667	<0.001
<b>Aulacanthidae Epipelagic</b>	Temperature	2.591	5.003	<0.001
$R_{adj}^2=0.394$	Salinity	1.523	1.789	0.002
	RFU	0.872	1.315	0.0042
	Bacteria	0.808	0.833	0.0160
	Primary Productivity	2.622	9.160	<0.001
	Particle Concentration	1.937	2.751	<0.001
<b>Aulacanthidae Upper Mesopelagic</b>	Avg C Flux	1.675	1.408	0.0109
$R_{adj}^2=0.132$	Particle Concentration	2.308	2.476	0.0013
<b>Aulacanthidae Lower Mesopelagic</b>	Avg Mass Flux	1.476	1.418	0.0076
$R_{adj}^2=0.308$	Particle Concentration	2.457	7.756	<0.001
<b>Aulosphaeridae Upper Mesopelagic</b>	Particle Concentration	2.778	12.76	<0.001
$R_{adj}^2=0.196$				
<b>Aulosphaeridae Lower Mesopelagic</b>	Particle Concentration	2.012	6.306	<0.001

Model	Term	edf	F	p
$R^2_{adj}=0.148$				
<b>Castanellidae Epipelagic</b>	Salinity	0.915	0.400	0.0935
$R^2_{adj}=0.228$	RFU	0.912	2.052	<0.001
	Si	2.018	3.656	<0.001
	Bacteria	1.128	0.883	0.0170
	Particle Concentration	2.278	4.028	<0.001
<b>Coelodendridae Upper Mesopelagic</b>	Avg N Flux	0.734	0.551	0.0527
$R^2_{adj}=0.09$	Particle Concentration	0.965	5.102	<0.001
<b>Coelodendridae Lower Mesopelagic</b>	Particle Concentration	3.051	6.768	<0.001
$R^2_{adj}=0.157$				
<b>Collodaria Epipelagic</b>	Salinity	0.926	2.267	<0.001
$R^2_{adj}=0.16$	O2	2.015	2.217	<0.001
	Bacteria	1.843	2.100	0.0024
<b>Foraminifera Epipelagic</b>	Temperature	4.420	7.624	<0.001
$R^2_{adj}=0.543$	O2	0.799	0.788	0.023
	Bacteria	0.000	0.000	0.523
	Avg N Flux	1.847	3.022	<0.001
	Primary Productivity	0.472	0.139	0.183
	Particle Concentration	1.685	2.955	<0.001

<sup>281</sup> In the upper mesopelagic (200-500m), abundances were generally low (Figure 4) so GAMs were only constructed for Acantharea, Aulacanthidae, Aulosphaeridae, and Coelodendridae (Table 2). All these models

had generally poor fits ( $R^2_{adj} < 0.20$ ). Yet, for all upper mesopelagic models, particle concentration was a significant explanatory variable (Table 2, Supplemental Figure 5). The lower mesopelagic also had generally poor GAM fits for taxon specific models ( $R^2_{adj} < 0.31$ ), with the exception of Acantharea ( $R^2_{adj} = 0.496$ ). Acantharea in the lower mesopelagic was most clearly positively associated with particle concentration (Supplemental Figure 6). For all Phaeodaria with a significant model, particle concentration was a main predictor variable (Table 2, Supplemental Figure 6).

## 289 Discussion

### 290 Overall Rhizaria abundance and patterns

291 In the epipelagic Rhizaria exhibited a notable seasonal pattern. Rhizaria abundances were higher in the  
292 summer months and lower during the winter. During a prior time period, Blanco-Bercial et al. (2022) noted  
293 that there is considerable seasonality in the community composition of all protists. Despite the seasonality  
294 of Rhizaria abundance, community composition was relatively consistent, with Collodaria representing the  
295 bulk of the community. It should be noted that the overall taxonomic resolution of the UVP5 is fairly  
296 low, so there may be a switching of species within the broad groups identified in this study which were not  
297 captured. Throughout the mesopelagic, month-to-month variation in 2021 was relatively low. Again, this is  
298 consistent with observations from metabarcoding of the whole protist community in the same study region  
299 (Blanco-Bercial et al., 2022). This finding is not surprising as the overall seasonal variation in environmental  
300 conditions in this region were low.

301 Overall Rhizaria were the most commonly identified group of mesoplankton throughout the study period.  
302 We do note that the UVP5 commonly captures *Trichodesmium* colonies, yet these were excluded in this  
303 comparison as they are strictly autotrophs. It should be noted that previous work has suggested that

304 avoidance behavior with the UVP is possible, at times likely, for visual and highly mobile zooplankton  
305 (Barth and Stone, 2022). Thus, the percent contribution reported here (42.7%) of Rhizaria to the total  
306 mesozooplankton community may be inflated due to under sampling of organisms such as Euphausiids and  
307 Chaetognaths which have quick escape responses. Regardless, it is worth noting that in the same region,  
308 with data collected in 2012 and 2013 using similar calculation methods, Biard et al. (2016) estimated large  
309 Rhizaria only contribute 15% of the total mesozooplankton community in the upper 500m. Likely, Rhizaria  
310 display considerable interannual variability. In the present study, we noticed considerably higher Rhizaria  
311 abundance throughout the water column in 2019 compared to 2021. Similarly, in the California Current a  
312 multi-year study of Aulosphaeridae saw considerable variation between years (Biard et al., 2018). To truly  
313 understand the drivers of interannual variability however, sustained observations of Rhizaria over longer time  
314 periods are required.

### 315 **Relationship to environmental parameters**

316 In general, the fit of most GAMs were moderate to poor. One possible reason for the poor fits may have  
317 been that for some taxa, conditions were not variable enough to capture a range of conditions at which  
318 they may exist. For instance, Collodaria were the most abundant taxa observed, yet the fit of their GAM  
319 was particularly poor. In studies which covered a wider range of parameters, Collodaria has been shown  
320 to strongly vary with changes in parameters such as temperature, chlorophyll-a, mixing, and water clarity  
321 (Biard et al., 2017; Biard and Ohman, 2020). Alternatively, Acantharea had relatively good fitting GAMs.  
322 These taxa also had some of the largest variation from month to month on cruises. Thus, it may be that  
323 in the oligotrophic, the relatively stable conditions can support certain taxa while others are more sporadic.  
324 It should also be noted that due to the challenge of adequately sampling enough volume to overcome low-  
325 detection issues, GAMs were run on integrated data. However, variation with environmental parameters

326 throughout the water column are likely, just not captured in the modelling aspect of this study. Future  
327 studies which are able to account for detection biases in finer vertical resolution of Rhizaria may improve  
328 ecological models of their abundance. One consistent parameter which had significant positive associations  
329 was particle concentration. This observation is not surprising as most Rhizaria likely to some extent engage  
330 in flux feeding.

331 **Vertical Structure and Trophic Roles**

332 In this study we present a clear pattern of vertical zonation between different Rhizaria groups. Largely, the  
333 taxonomic composition and vertical positioning were similar to Rhizaria zonation in the California Current  
334 Ecosystem (Biard and Ohman, 2020). It should be noted however, that the secondary abundance peak  
335 reported in the present study is lower. This is likely due to the more oligotrophic nature of the study region,  
336 where the euphotic zone penetrates deeper into the water column. Most prevalent in the epipelagic were  
337 Collodaria. These mixotrophic Radiolaria have long been reported to contribute to primary productivity in  
338 the euphotic zone (Dennett et al., 2002; Michaels et al., 1995). Collodaria are thought to be particularly  
339 successful globally in oligotrophic regions due to their photosymbiotic relationships (Biard et al., 2017, 2016).  
340 We observed the highest abundance of Collodaria during June 2021, supporting the notion they can thrive  
341 during the typically low-nutrient conditions of summer stratification. However, Collodaria also increased  
342 during the spring mixing period, suggesting that they can thrive during conditions which may typically be  
343 thought to favor autotrophs. Furthermore, while Collodaria were primarily absent from below 250m, there  
344 were a few instances of deeper colonies being observed. Global investigations of polycystine flux, suggest  
345 that deep-Collodaria in oligotrophic regions may be a consequence of isothermal submersion (Boltovskoy,  
346 2017). Alternatively, surface waters at BATS often mix into the mode water during the seasonal mixing,  
347 so Collodaria in the deeper waters may be a result of diapycnal mixing. Another effectively exclusively

348 epipelagic Rhizaria was the Phaeodaria family of Castanellidae. All Phaeodaria are thought to be fully  
349 heterotrophic (Nakamura and Suzuki, 2015), nonetheless a number of studies, including this one, report  
350 Castanellidae to be typically found in the lower epipelagic (Biard et al., 2018; Biard and Ohman, 2020;  
351 Zasko and Rusanov, 2005). It should be considered that perhaps Castanellidae specializes in feeding on  
352 sinking particles directly at the base of the epipelagic. Given it's smaller size (Nakamura and Suzuki, 2015),  
353 Castanellidae does not need a large diameter to efficiently flux feed at the typically particle rich region of  
354 the lower epipelagic.

355 The mesopelagic generally was home to known heterotrophic organisms, particularly for those which were  
356 constrained to exclusively occupy deeper waters. This is consistent with Blanco-Bercial et al. (2022)'s  
357 observation of an auto-/mixotroph to heterotroph gradient in local protist community as well as global  
358 patterns in Rhizaria ecology [Laget et al. (2024)]. The upper mesopelagic interestingly had relatively  
359 low total abundance. This low-abundance region likely reflects the dynamics of productivity and export  
360 throughout the water column. While productivity and thus sinking particles for flux feeders are high in the  
361 euphotic zone, much of this is attenuated throughout the epipelagic. So, while the base of the epipelagic  
362 may provide a rich feeding environment for Castanellidae, smaller protists, or heterotrophic bacteria (Figure  
363 2F), the region from 200-500m might be otherwise food poor. Perhaps it is more advantageous for Rhizaria  
364 to situate deeper, in darker regions of the twilight zone where visual predators and vertically migrating  
365 organisms may not feed on them. Also it should be noted that Phaeodaria utilize silica to build their  
366 opaline tests, and silica concentrations started to increase around 500m (Figure 2G). However, *Si* was not  
367 a significant term for any taxon-specific model in the mesopelagic. Aulosphaeridae was only found to have  
368 significant relationships, although weak fits, to particle concentration in the mesopelagic. In our study,  
369 while consistently observed, overall abundances of Aulosphaeridae were very low. In the Pacific Ocean,  
370 on California's Coast, much higher abundances of Aulosphaeridae have been reported [Zasko and Rusanov

371 (2005); Biard and Ohman (2020)] and they have massive potential to impact silica export (Biard et al.,  
372 2018). Coelodendrididae were also seemingly restricted to the deeper section of the mesopelagic. This is  
373 interesting given that in the California Current, (Biard and Ohman, 2020) found a bimodal distribution in  
374 Coelodendrididae. There are several morphotypes corresponding to different taxa of Coelodendrididae (Biard  
375 and Ohman, 2020; Nakamura and Suzuki, 2015). So it may be that only a few types of Coelodendrididae  
376 were observed in this study, while the epipelagic variety was not. Alternatively, the lower epipelagic of the  
377 extremely productive California Current may provide adequate habitat for Coelodendrididae, which is not  
378 available in the oligotrophic Sargasso Sea.

379 A number of taxa were found to have a bimodal distribution, with sizable populations in both the epipelagic  
380 and mesopelagic. Aulacanthidae had a bimodal distribution, although abundances were highest in the lower  
381 mesopelagic. Foraminifera also had a bimodal distribution. Some lineages of Foraminifera are known to  
382 host photosymbionts (Biard, 2022a; Kimoto, 2015), however they are also efficient predators commonly seen  
383 throughout the mesopelagic (Caron and Be, 1984; Gaskell et al., 2019). Thus it is not surprising to find  
384 their presence in both locations of the water column. Foraminifera are also known to vary their vertical  
385 distribution across their life cycle in phase with lunar cycles (Biard, 2022a; Bijma et al., 1990; Gaskell et al.,  
386 2019; Kimoto, 2015). However, the sampling scheme of the BATS program does not capture this frequency  
387 and was not investigated in the present study.

388 Acantharea also had a bimodal distribution, with much more sizable abundances than Aulacanthidae or  
389 Foraminifera. Most prior studies of Acantharea vertical distribution found them concentrated in near sur-  
390 face layers of the water column Zasko and Rusanov (2005). This would support the paradigm that large  
391 Acantharea abundances may be supported by their mixotrophic abilities (Michaels et al., 1995; Suzuki and  
392 Not, 2015). While the UVP5 images cannot distinguish between mixotrophic and heterotrophic Acantharea,  
393 the GAMs constructed for Acantharea abundance found positive associations with particle concentration

and mass flux, suggesting a higher reliance on heterotrophy. Recently Mars Brisbin et al. (2020) described apparent predator behavior amongst near-surface Acantharea. Thus it is likely that epipelagic Acantharea may commonly be heterotrophic or mixotrophic with an increased reliance on heterotrophy. Yet, it should be noted in the Sargasso Sea, both heterotrophic and symbiotic lineages of Acantharea have been reported (Blanco-Bercial et al., 2022). Additionally, Michaels (1988) noted that the majority of Acantharea (by abundance) were smaller than  $160\mu m$ . While that estimate may be inflated due to inability to capture larger cells, small Acantharea were not captured in the present study. Thus, trophic strategy may shift based on sizes of Acantharea.

Decelle et al. (2013) proposed a hypothetical life cycle for cyst-bearing (strictly heterotrophic) Acantharea. This hypothesized life cycle suggests that epipelagic Acantharea are adult populations, which form cysts that sink into the mesopelagic, then reproduce and rise. Furthermore, given that horizontal transfer of symbionts between generations of Acantharea is unlikely due to their spawning behavior, the newly spawned mesopelagic Acantharea are not necessarily required to rapidly return to the photic zone (Decelle et al., 2013, 2012). This hypothesis predicts that Acanthareas in the mesopelagic would be smaller (Decelle et al., 2013). Mars Brisbin et al. (2020) provided some support for this hypothesis, with a significant decrease in Acantharea sizes with depth. Although the authors also observed low abundances in the mesopelagic and noted that the smaller sizes may be due to lower food availability (Mars Brisbin et al., 2020). Since food is more scarce in the mesopelagic, nutritional quality lower, yet flux feeders would likely grow larger to increase their feeding range (Biard and Ohman, 2020; Stukel et al., 2018). In the data collecting in this study, Acanthareas in the mesopelagic were significantly smaller than the epipelagic, despite the other bimodal taxa (Foraminifera and Aulacanthidae) being significantly larger with depth. This provides added support for the hypothesis that cyst-forming Acantharea may utilize different sections of the water column throughout their life cycle. However to further investigate this, more work is needed with higher temporal

<sup>417</sup> and taxonomic resolution.

<sup>418</sup> **Conclusions and Considerations**

<sup>419</sup> This study provides a detailed look at Rhizaria abundance over time throughout the water column in a  
<sup>420</sup> major oligotrophic gyre. We show that their abundances are generally related to particle concentration and  
<sup>421</sup> flux, although lack of environmental variability may have reduced the fit of our GAMs. Considering the  
<sup>422</sup> potential role of Rhizaria in the biological carbon pump, they may have a somewhat mixed role. In the  
<sup>423</sup> shallower regions, they may be an attenuating force on sinking particles (Stukel et al., 2019). However,  
<sup>424</sup> once consumed and repackaged by larger Rhizaria, they can sink quicker and contribute more to overall flux  
<sup>425</sup> (Michaels, 1988). Thus, Rhizaria may act as an aggregation mechanism. However, to truly test this, more  
<sup>426</sup> work is needed measuring Rhizaria flux.

<sup>427</sup> The vertical partitioning documented in this study do support the hypothesis that mixotrophic rhizaria will  
<sup>428</sup> occupy shallower waters while deeper waters are dominated by heterotrophy. However the degree to which  
<sup>429</sup> mixotrophic Rhizaria in the euphotic zone rely on heterotrophy versus symbiosis is uncertain. Collodaria  
<sup>430</sup> were recorded as consistent and dominant members of the near surface region. These organisms have the  
<sup>431</sup> potential to contribute considerably to the otherwise low productivity of oligotrophic regions. However, their  
<sup>432</sup> role in food webs is not well understood. While this study represents a step-forward in our understanding  
<sup>433</sup> of Rhizaria ecology, continued research on Rhizaria is much needed to better understand their ecology.  
<sup>434</sup> Particularly extended work describing interannual patterns in Rhizaria abundance. Also work defining  
<sup>435</sup> biotic interactions, feeding rates, productivity, and life history are all rich fields of interest in Rhizaria.

436    **References:**

- 437    Anderson, O.R., 2014. Living Together in the Plankton: A Survey of Marine Protist Symbioses. *Acta*  
438    *Protozoologica* 53, 29–38. <https://doi.org/10.4467/16890027AP.13.0019.1116>
- 439    Anderson, O.R., Bé, A.W.H., 1976. A CYTOCHEMICAL FINE STRUCTURE STUDY OF PHAGOTRO-  
440    PHY IN A PLANKTONIC FORAMINIFER, *HASTIGERINA PELAGICA* (d'ORBIGNY). *The Biological*  
441    *Bulletin* 151, 437–449. <https://doi.org/10.2307/1540498>
- 442    Barth, A., Stone, J., 2024. Understanding the picture: The promises and challenges of in-situ imagery data in  
443    the study of plankton ecology. *Journal of Plankton Research: Horizons* 1–15. <https://doi.org/10.1093/plankt/fbae023>
- 444    Barth, A., Stone, J., 2022. Comparison of an in situ imaging device and net-based method to study meso-  
445    zooplankton communities in an oligotrophic system. *Frontiers in Marine Science* 9.
- 446    Benfield, M.C., Davis, C.S., Wiebe, P.H., Gallager, S.M., Gregory Lough, R., Copley, N.J., 1996. Video  
447    Plankton Recorder estimates of copepod, pteropod and larvacean distributions from a stratified region  
448    of Georges Bank with comparative measurements from a MOCNESS sampler. *Deep Sea Research Part*  
449    *II: Topical Studies in Oceanography* 43, 1925–1945. [https://doi.org/10.1016/S0967-0645\(96\)00044-6](https://doi.org/10.1016/S0967-0645(96)00044-6)
- 450    Biard, T., 2022a. Rhizaria. *Encyclopeida of Life Sciences*, pp. 1–11. <https://doi.org/10.1002/9780470015902.a0029469>
- 451    Biard, T., 2022b. Diversity and ecology of Radiolaria in modern oceans. *Environmental Microbiology* 24,  
452    2179–2200. <https://doi.org/10.1111/1462-2920.16004>
- 453    Biard, T., Bigeard, E., Audic, S., Poulain, J., Gutierrez-Rodriguez, A., Pesant, S., Stemmann, L., Not, F.,  
454    2017. Biogeography and diversity of Collodaria (Radiolaria) in the global ocean. *The ISME Journal* 11,  
455    1331–1344. <https://doi.org/10.1038/ismej.2017.12>
- 456    Biard, T., Krause, J.W., Stukel, M.R., Ohman, M.D., 2018. The Significance of Giant Phaeodarians

- 459 (Rhizaria) to Biogenic Silica Export in the California Current Ecosystem. Global Biogeochemical Cy-  
460 cles 32, 987–1004. <https://doi.org/10.1029/2018GB005877>
- 461 Biard, T., Ohman, M.D., 2020. Vertical niche definition of test-bearing protists (Rhizaria) into the twilight  
462 zone revealed by in situ imaging. Limnology and Oceanography 65, 2583–2602. <https://doi.org/10.1002/lno.11472>
- 463
- 464 Biard, T., Stemmann, L., Picheral, M., Mayot, N., Vandromme, P., Hauss, H., Gorsky, G., Guidi, L., Kiko,  
465 R., Not, F., 2016. In situ imaging reveals the biomass of giant protists in the global ocean. Nature 532,  
466 504–507. <https://doi.org/10.1038/nature17652>
- 467 Bijma, J., Erez, J., Hemleben, C., 1990. **Lunar and semi-lunar reproductive cycles in some spinose planktonic**  
468 **foraminifers**. Journal of Foraminiferal Research 20, 117–127.
- 469 Blanco-Bercial, L., 2020. **Metabarcoding analyses and seasonality of the zooplankton community at BATS**.  
470 Frontiers in Marine Science 7.
- 471 Blanco-Bercial, L., Parsons, R., Bolaños, L.M., Johnson, R., Giovannoni, S.J., Curry, R., 2022. **The pro-**  
472 **tist community traces seasonality and mesoscale hydrographic features in the oligotrophic sargasso sea**.  
473 Frontiers in Marine Science 9.
- 474 Boltovskoy, D., 2017. Vertical distribution patterns of radiolaria polycystina (protista) in the world ocean:  
475 Living ranges, isothermal submersion and settling shells. Journal of Plankton Research 39, 330–349.  
476 <https://doi.org/10.1093/plankt/fbx003>
- 477 Boltovskoy, D., Alder, V.A., Abelmann, A., 1993. Annual flux of radiolaria and other shelled plankters in  
478 the eastern equatorial atlantic at 853 m: seasonal variations and polycystine species-specific responses.  
479 Deep Sea Research Part I: Oceanographic Research Papers 40, 1863–1895. [https://doi.org/10.1016/0967-0637\(93\)90036-3](https://doi.org/10.1016/0967-0637(93)90036-3)
- 480
- 481 Caron, D.A., 2016. **The rise of rhizaria | nature**. Nature 532, 444–445.

- 482 Caron, D.A., Be, A.W.H., 1984. PREDICTED AND OBSERVED FEEDING RATES OF THE SPINOSE  
483 PLANKTONIC FORAMINIFER. BULLETIN OF MARINE SCIENCE 35.
- 484 Caron, D.A., Michaels, A.F., Swanberg, N.R., Howse, F.A., 1995. Primary productivity by symbiont-bearing  
485 planktonic sarcodines (acantharia, radiolaria, foraminifera) in surface waters near bermuda. Journal of  
486 Plankton Research 17, 103–129. <https://doi.org/10.1093/plankt/17.1.103>
- 487 Cohen, N.R., Krinos, A.I., Kell, R.M., Chmiel, R.J., Moran, D.M., McIlvin, M.R., Lopez, P.Z., Barth, A.,  
488 Stone, J., Alanis, B.A., Chan, E.W., Breier, J.A., Jakuba, M.V., Johnson, R., Alexander, H., Saito, M.A.,  
489 2023. Microeukaryote metabolism across the western North Atlantic Ocean revealed through autonomous  
490 underwater profiling. <https://doi.org/10.1101/2023.11.20.567900>
- 491 Decelle, J., Colin, S., Foster, R.A., 2015. Photosymbiosis in Marine Planktonic Protists, in: Ohtsuka, S.,  
492 Suzuki, T., Horiguchi, T., Suzuki, N., Not, F. (Eds.), Springer Japan, Tokyo, pp. 465–500. [https://doi.org/10.1007/978-4-431-55130-0\\_19](https://doi.org/10.1007/978-4-431-55130-0_19)
- 493 Decelle, J., Martin, P., Paborstava, K., Pond, D.W., Tarling, G., Mahé, F., De Vargas, C., Lampitt, R.,  
494 Not, F., 2013. Diversity, Ecology and Biogeochemistry of Cyst-Forming Acantharia (Radiolaria) in the  
495 Oceans. PLoS ONE 8, e53598. <https://doi.org/10.1371/journal.pone.0053598>
- 496 Decelle, J., Siano, R., Probert, I., Poirier, C., Not, F., 2012. Multiple microalgal partners in symbiosis  
497 with the acantharian *Acanthochiasma* sp. (Radiolaria). Symbiosis 58, 233–244. <https://doi.org/10.1007/s13199-012-0195-x>
- 498 Dennett, M.R., Caron, D.A., Michaels, A.F., Gallager, S.M., Davis, C.S., 2002. Video plankton recorder  
499 reveals high abundances of colonial radiolaria in surface waters of the central north pacific. Journal of  
500 Plankton Research 24, 797–805. <https://doi.org/10.1093/plankt/24.8.797>
- 501 Drago, L., Panaïotis, T., Irisson, J.-O., Babin, M., Biard, T., Carlotti, F., Coppola, L., Guidi, L., Hauss, H.,  
502 Karp-Boss, L., Lombard, F., McDonnell, A.M.P., Picheral, M., Rogge, A., Waite, A.M., Stemmann, L.,

- 505 Kiko, R., 2022. Global Distribution of Zooplankton Biomass Estimated by In Situ Imaging and Machine  
506 Learning. *Frontiers in Marine Science* 9. <https://doi.org/10.3389/fmars.2022.894372>
- 507 Gaskell, D.E., Ohman, M.D., Hull, P.M., 2019. Zooglider-based measurements of planktonic foraminifera in  
508 the California Current System. *Journal of Foraminiferal Research* 49, 390–404. <https://doi.org/10.2113/gsjfr.49.4.390>
- 510 Gorsky, G., Ohman, M.D., Picheral, M., Gasparini, S., Stemmann, L., Romagnan, J.-B., Cawood, A., Pesant,  
511 S., García-Comas, C., Prejger, F., 2010. Digital zooplankton image analysis using the ZooScan integrated  
512 system. *Journal of Plankton Research* 32, 285–303. <https://doi.org/10.1093/plankt/fbp124>
- 513 Gowing, M.M., 1989. Abundance and feeding ecology of Antarctic phaeodarian radiolarians. *Marine Biology*  
514 103, 107–118. <https://doi.org/10.1007/BF00391069>
- 515 Gutierrez-Rodriguez, A., Stukel, M.R., Lopes dos Santos, A., Biard, T., Scharek, R., Vaulot, D., Landry,  
516 M.R., Not, F., 2019. High contribution of Rhizaria (Radiolaria) to vertical export in the California  
517 Current Ecosystem revealed by DNA metabarcoding. *The ISME Journal* 13, 964–976. <https://doi.org/10.1038/s41396-018-0322-7>
- 519 Gutiérrez-Rodríguez, A., Lopes dos Santos, A., Safi, K., Probert, I., Not, F., Fernández, D., Gourvil, P.,  
520 Bilewitch, J., Hulston, D., Pinkerton, M., Nodder, S.D., 2022. Planktonic protist diversity across con-  
521 trasting subtropical and subantarctic waters of the southwest Pacific. *Progress in Oceanography* 206,  
522 102809. <https://doi.org/10.1016/j.pocean.2022.102809>
- 523 Haekel, E., 1887. *Report on the radiolaria collected by H.M.S. Challenger during the years 1873-1876, plates,*  
524 *by Ernst Haeckel.*
- 525 Hull, P.M., Osborn, K.J., Norris, R.D., Robison, B.H., 2011. Seasonality and depth distribution of a  
526 mesopelagic foraminifer, *Hastigerinella digitata*, in Monterey Bay, California. *Limnology and Oceanog-  
527 raphy* 56, 562–576. <https://doi.org/10.4319/lo.2011.56.2.0562>

- 528 Ikenoue, T., Kimoto, K., Okazaki, Y., Sato, M., Honda, M.C., Takahashi, K., Harada, N., Fujiki, T., 2019.
- 529     Phaeodaria: An Important Carrier of Particulate Organic Carbon in the Mesopelagic Twilight Zone
- 530     of the North Pacific Ocean. *Global Biogeochemical Cycles* 33, 1146–1160. <https://doi.org/10.1029/2019GB006258>
- 532 Kimoto, K., 2015. Planktic foraminifera. pp. 129–178. [https://doi.org/10.1007/978-4-431-55130-0\\_7](https://doi.org/10.1007/978-4-431-55130-0_7)
- 533 Knap, A.H., Michaels, A.F., Steinberg, D.K., Bahr, F., Bates, N.R., Bell, S., Countway, P., Close, A.R.,
- 534 Doyle, A.P., Dow, R.L., Howse, F.A., Gundersen, K., Johnson, R.J., Kelly, R., Little, R., Orcutt, K.,
- 535 Parsons, R., Rathburn, C., Sanderson, M., Stone, S., 1997. **BATS methods manual, version 4**.
- 536 Laget, M., Drago, L., Panaïotis, T., Kiko, R., Stemmann, L., Rogge, A., Llopis-Monferrer, N., Leynaert,
- 537 A., Irisson, J.-O., Biard, T., 2024. Global census of the significance of giant mesopelagic protists to the
- 538 marine carbon and silicon cycles. *Nature Communications* 15, 3341. <https://doi.org/10.1038/s41467-024-47651-4>
- 540 Lee, J.J., 2006. **Algal symbiosis in larger foraminifera**. *Symbiosis* 42, 63–75.
- 541 Llopis Monferrer, N., Biard, T., Sandin, M.M., Lombard, F., Picheral, M., Elineau, A., Guidi, L., Leynaert,
- 542 A., Tréguer, P.J., Not, F., 2022. **Siliceous rhizaria abundances and diversity in the mediterranean sea**
- 543 **assessed by combined imaging and metabarcoding approaches**. *Frontiers in Marine Science* 9.
- 544 Lomas, M.W., Bates, N.R., Johnson, R.J., Knap, A.H., Steinberg, D.K., Carlson, C.A., 2013. Two decades
- 545 and counting: 24-years of sustained open ocean biogeochemical measurements in the Sargasso Sea. *Deep*
- 546 *Sea Research Part II: Topical Studies in Oceanography* 93, 16–32. <https://doi.org/10.1016/j.dsr2.2013.01.008>
- 547 Lombard, F., Boss, E., Waite, A.M., Vogt, M., Uitz, J., Stemmann, L., Sosik, H.M., Schulz, J., Romagnan,
- 549 J.-B., Picheral, M., Pearlman, J., Ohman, M.D., Niehoff, B., Möller, K.O., Miloslavich, P., Lara-Lpez,
- 550 A., Kudela, R., Lopes, R.M., Kiko, R., Karp-Boss, L., Jaffe, J.S., Iversen, M.H., Irisson, J.-O., Fennel,

- 551 K., Hauss, H., Guidi, L., Gorsky, G., Giering, S.L.C., Gaube, P., Gallager, S., Dubelaar, G., Cowen,  
552 R.K., Carlotti, F., Briseño-Avena, C., Berline, L., Benoit-Bird, K., Bax, N., Batten, S., Ayata, S.D., Ar-  
553 tigas, L.F., Appeltans, W., 2019. [Globally consistent quantitative observations of planktonic ecosystems](#).  
554 Frontiers in Marine Science 6.
- 555 Marra, G., Wood, S.N., 2011. Practical variable selection for generalized additive models. Computational  
556 Statistics & Data Analysis 55, 2372–2387. <https://doi.org/10.1016/j.csda.2011.02.004>
- 557 Mars Brisbin, M., Brunner, O.D., Grossmann, M.M., Mitarai, S., 2020. Paired high-throughput, in situ  
558 imaging and high-throughput sequencing illuminate acantharian abundance and vertical distribution.  
559 Limnology and Oceanography 65, 2953–2965. <https://doi.org/10.1002/lno.11567>
- 560 McGillicuddy, D.J., Robinson, A.R., Siegel, D.A., Jannasch, H.W., Johnson, R., Dickey, T.D., McNeil, J.,  
561 Michaels, A.F., Knap, A.H., 1998. Influence of mesoscale eddies on new production in the Sargasso Sea.  
562 Nature 394, 263–266. <https://doi.org/10.1038/28367>
- 563 Michaels, A.F., 1988. Vertical distribution and abundance of Acantharia and their symbionts. Marine  
564 Biology 97, 559–569. <https://doi.org/10.1007/BF00391052>
- 565 Michaels, A.F., Caron, D.A., Swanberg, N.R., Howse, F.A., Michaels, C.M., 1995. Planktonic sarcodines  
566 (Acantharia, Radiolaria, Foraminifera) in surface waters near Bermuda: abundance, biomass and vertical  
567 flux. Journal of Plankton Research 17, 131–163. <https://doi.org/10.1093/plankt/17.1.131>
- 568 Michaels, A.F., Knap, A.H., 1996. Overview of the U.S. JGOFS Bermuda Atlantic Time-series Study and  
569 the Hydrostation S program. Deep Sea Research Part II: Topical Studies in Oceanography 43, 157–198.  
570 [https://doi.org/10.1016/0967-0645\(96\)00004-5](https://doi.org/10.1016/0967-0645(96)00004-5)
- 571 Nakamura, Y., Itagaki, H., Tuji, A., Shimode, S., Yamaguchi, A., Hidaka, K., Ogiso-Tanaka, E., 2023.  
572 DNA metabarcoding focused on difficult-to-culture protists: An effective approach to clarify biological  
573 interactions. Environmental Microbiology 25, 3630–3638. <https://doi.org/10.1111/1462-2920.16524>

- 574 Nakamura, Y., Suzuki, N., 2015. [Phaeodaria: Diverse marine cercozoans of world-wide distribution](#).  
575 Springer, pp. 223–249.
- 576 Ohman, M.D., 2019. A sea of tentacles: optically discernible traits resolved from planktonic organisms in  
577 situ. ICES Journal of Marine Science 76, 1959–1972. <https://doi.org/10.1093/icesjms/fsz184>
- 578 Panaïotis, T., Babin, M., Biard, T., Carlotti, F., Coppola, L., Guidi, L., Hauss, H., Karp-Boss, L., Kiko, R.,  
579 Lombard, F., McDonnell, A.M.P., Picheral, M., Rogge, A., Waite, A.M., Stemmann, L., Irisson, J.-O.,  
580 2023. Three major mesoplanktonic communities resolved by in situ imaging in the upper 500 m of the  
581 global ocean. Global Ecology and Biogeography 32, 1991–2005. <https://doi.org/10.1111/geb.13741>
- 582 Picheral, M., Colin, S.P., Irisson, J.-O., n.d. [Ecotaxa](#).
- 583 Picheral, M., Guidi, L., Stemmann, L., Karl, D.M., Iddaoud, G., Gorsky, G., 2010. The Underwater  
584 Vision Profiler 5: An advanced instrument for high spatial resolution studies of particle size spectra  
585 and zooplankton. Limnology and Oceanography: Methods 8, 462–473. <https://doi.org/10.4319/lom.2010.8.462>
- 586
- 587 Sogawa, S., Nakamura, Y., Nagai, S., Nishi, N., Hidaka, K., Shimizu, Y., Setou, T., 2022. DNA metabarcod-  
588 ing reveals vertical variation and hidden diversity of alveolata and rhizaria communities in the west-  
589 ern north pacific. Deep Sea Research Part I: Oceanographic Research Papers 183, 103765. <https://doi.org/10.1016/j.dsr.2022.103765>
- 590
- 591 Stukel, M.R., Biard, T., Krause, J., Ohman, M.D., 2018. Large Phaeodaria in the twilight zone: Their role  
592 in the carbon cycle. Limnology and Oceanography 63, 2579–2594. <https://doi.org/10.1002/lno.10961>
- 593 Stukel, M.R., Ohman, M.D., Kelly, T.B., Biard, T., 2019. [The roles of suspension-feeding and flux-feeding](#)  
594 [zooplankton as gatekeepers of particle flux into the mesopelagic ocean in the northeast pacific](#). Frontiers  
595 in Marine Science 6.
- 596 Suzuki, N., Not, F., 2015. [Biology and ecology of radiolaria](#). Springer, pp. 179–222.

- 597 Swanberg, N.R., Anderson, O.R., 1981. Collozoum caudatum sp. nov.: A giant colonial radiolarian from  
598 equatorial and Gulf Stream waters. Deep Sea Research Part A. Oceanographic Research Papers 28,  
599 1033–1047. [https://doi.org/10.1016/0198-0149\(81\)90016-9](https://doi.org/10.1016/0198-0149(81)90016-9)
- 600 Takahashi, K., Hurd, D.C., Honjo, S., 1983. Phaeodarian skeletons: Their role in silica transport to the  
601 deep sea. Science 222, 616–618. <https://doi.org/10.1126/science.222.4624.616>
- 602 Whitmore, B.M., Ohman, M.D., 2021. Zooglider-measured association of zooplankton with the fine-scale  
603 vertical prey field. Limnology and Oceanography 66, 3811–3827. <https://doi.org/10.1002/lno.11920>
- 604 Wood, S.N., 2017. Generalized additive models: an introduction with R, Second edition. ed, Texts in  
605 statistical science. CRC Press/Taylor & Francis Group, Boca Raton London New York.
- 606 Wood, S.N., 2001. mgcv: GAMs and Generalized Ridge Regression for R 1.
- 607 Zasko, D.N., Rusanov, I.I., 2005. Vertical Distribution of Radiolarians and Their Role in Epipelagic Com-  
608 munities of the East Pacific Rise and the Gulf of California. Biology Bulletin 32, 279–287. <https://doi.org/10.1007/s10525-005-0103-5>